1676 *Macromolecules* **1992,** *25,* 1676–1685

Theory of the Homopolymer/Binary-Polymer-Mixture Interface

Eugene Helfand

AT&T Bell Laboratories, Murray Hill, New Jersey 07974

Received September 11, 1991; Revised Manuscript Received November 20, 1991

ABSTRACT: A theory is developed to describe an interface that on one side has a pure polymer A and on the other side has a mixture of polymers B and C. In general one of the polymers, say B, adsorbs to the interface and significantly modifies properties such as interfacial tension and overlap of the A with the BC phase. Judicious choice of component B may thus lead to a desirable change from the properties of an A/C interface. Such changes may improve joint strength or slow the process of phase demixing, for example. Physical properties are calculated for interfaces with various values for the physical parameters. Trends observed in the data are discussed in physical terms. Adsorption is significant even with rather mild differences of interaction parameter or with a fairly small amount of B. This is because the homogenizing effect of entropy of mixing is insignificant with polymers and also because polymeric interfaces are broad. However, when one particular relation among the parameters holds, there is no adsorption to the interfacial region. The properties of such interfaces are given in closed form.

I. Introduction

The properties of the interfaces between polymeric phases are important in determining the nature of blends and of block copolymers. In earlier work[1–4] it was shown that such interfaces are frequently much broader than those of typical monomeric systems. This enhances entanglement and the strength of the joint. Also the interfacial tensions between immiscible polymers may be quite low, so that the driving force to growth of phase domains is small. This (together with low diffusion constants) accounts for the kinetic stability of intimate blends of polymeric phases.

Today the trend is to the use of more complex polymeric phases, including true thermodynamic mixtures. This makes worthwhile a study of the interface A/BC, by which we mean the interface between a pure polymeric phase A on one side and a mixture of polymers B and C on the other. Among the specific reasons for studying such an interface are the following:

(i) The interface may be part of a system chosen, for other reasons, to have this phase structure.

(ii) One may want to know how the addition of polymer C to a B phase can benefit the interfacial properties.

(iii) The methods and insights developed here will be useful in understanding even more complex interfaces, such as AB/CD, AB/BC, or interfaces containing block copolymers.

Under most circumstances one of the polymers of the BC mixture penetrates more deeply into the A phase than the other. The borderline condition where this deeper penetrating polymer changes from one component of the mixture to the other will be given, and this case examined.

In the system under consideration (according to the model we will use) four important parameters are the three Flory[5] parameters, χ_{AB}, χ_{AC}, and χ_{BC} (note that χ_{BC} must be negative for mixing of B and C to occur) and the volume fraction of B in the asymptotic mixture phase, $\phi_{B\infty}$. One of these (we will choose it to be χ_{AB}) serves only to scale distances, interfacial tensions, and the other χ's. Parameters also involved only in scaling (i.e., as multiplicative factors) are the statistical segment length, b, the pure polymer density, ρ_0, and the temperature, T.

The major thrust of our work has been to solve numerically equations describing the A/BC interface, in order to calculate the concentration profiles, interfacial tension, overlap of the phases, and adsorption of B to the interfacial region. However, the way properties change as the interaction and composition parameters are varied can frequently be qualitatively understood on more physical grounds, as we shall show.

In the next section we provide details about the model we will be using. Also we define the Gibbs dividing surface and surface excess (adsorption) of B. A review is presented then of the results of earlier studies of the simpler A/B interface. In section IV first the theory of the A/B interface is summarized as background, and then the theory appropriate for the A/BC interface is detailed (reading of this section is not essential for understanding the rest of the paper, specifically the results of the calculations of properties). In section V we look at the concentration profiles of B and C well into the region that is predominantly A. In section VI a discussion is presented of two limiting cases. One is when the parameters are such that the ratio of B to C remains constant everywhere. The other is when C is strongly repelled from overlap with A. The results of the calculation of the physical properties of the interface, as the parameters are varied, are given in section VII. A summary ends the body of the paper. Most of the analytic and numerical details are put into the appendices. Appendix A explains how the solutions of the equations behave as $x \to \pm\infty$ and the importance of getting this asymptotic behavior right in order to obtain a numerical solution of the differential equations. Appendices B and C provide details about the two limiting cases introduced in section VI.

Three-component, or quasi-three-component, polymeric interfaces that have previously been studied theoretically include two immiscible polymers that are compressible,[1] so that the third component is vacuum, or equivalently a neutral solvent; a homopolymer in two solvents that are only partially miscible;[6] and a block copolymer AB in the interface A/B.[7] In refs 6 and 7 the random phase approximation is used. All these references use perturbation techniques that limit their range of applicability.

II. The Model and Its Thermodynamics

Consider the interface that forms between two phases. One is pure polymer A. The other is a mixture of polymers B and C, with volume fraction $\phi_{B\infty}$ of B and $\phi_{C\infty} = 1 - \phi_{B\infty}$ of C. We will conventionally regard the A phase as being on the left, i.e., extending to $x \to -\infty$. Because the molecular weights of all the polymers will be taken as infinite, the A phase is pure, and the concentration of A falls to

0024-9297/92/2225-1676$03.00/0

zero as one moves to $x \to \infty$. For the A/B interface the asymptotic limit is effectively reached at fairly low degrees of polymerization,[8,9] typically $O(10)$. What is required is that the product of N and the smallest interaction parameter be large compared with unity.

For simplicity, certain properties of the pure polymers A, B, and C will be taken as the same: viz., the density when pure, ρ_0, in monomers per unit volume; and the statistical length of a monomer, b. This assumption was easily removed in the case of the A/B interface[2] and presumably can be removed here, too. The surface tension depends only on the combination variable, $\rho_0 b^2$, which is much closer to being constant for most polymers than the individual factors.

The interactions are characterized by χ parameters such that the interaction free energy density (excluding gradient terms that are generally negligible[2]) is

$$f/\rho_0 k_B T = \chi_{AB}\phi_A\phi_B + \chi_{AC}\phi_A\phi_C + \chi_{BC}\phi_B\phi_C \qquad (2.1)$$

For the present system χ_{AB} and χ_{AC} are positive, while χ_{BC} is negative.

We will need the chemical potentials of the components relative to the pure materials. These are obtained from the conditions in the asymptotic phases and are given by[5]

$$\Delta\mu_B/k_B T = \chi_{BC}\phi_{C\infty}^2 \qquad (2.2)$$

$$\Delta\mu_C/k_B T = \chi_{BC}\phi_{B\infty}^2 \qquad (2.3)$$

The interface is characterized by the density profiles $\phi_A(x)$, $\phi_B(x)$, and $\phi_C(x)$, these being nontrivial in the region near $x = 0$. The plane to be called $x = 0$ is arbitrary. We will select it as the Gibbs dividing surface for component A, i.e., the level of x such that the amount of A material in the right half-space exactly equals the deficit of A in the left half-space:

$$\int_0^\infty dx\, \phi_A(x) = \int_{-\infty}^0 dx\, [1 - \phi_A(x)] \qquad (2.4)$$

The differential absorption to the interface of the components of the mixed phase can be characterized by a quantity n_{xsB}, the excess B in the surface region (in monomers per unit area)

$$n_{xsB} = \rho_0\left\{\int_{-\infty}^0 dx\, \phi_B(x) + \int_0^\infty dx\, [\phi_B(x) - \phi_{B\infty}]\right\} \qquad (2.5)$$

III. Review of the A/B Interfacial Properties

The present paper is an extension of the theory of the A/B interface, as developed by Helfand and Tagami.[1] In this section we will summarize the results of that study. Later we present a brief review of the theoretical basis.

The interfacial tension, γ, of the A/B interface is given by

$$\gamma = 6^{-1/2} k_B T \rho_0 b \chi_{AB}^{1/2} \qquad (3.1)$$

The interfacial profiles of A and B are

$$\phi_A(x) = \frac{1}{2}\left\{1 - \tanh\left[\frac{(6\chi_{AB})^{1/2}}{b}x\right]\right\} \qquad (3.2)$$

$$\phi_B(x) = 1 - \phi_A(x) \qquad (3.3)$$

Hence one measure of the characteristic thickness of the interface is $a_I = b/(6\chi_{AB})^{1/2}$. Since χ_{AB} can be quite small, the thickness of the interface can be quite a bit larger than that between small-molecule phases. Their are many ways (differing by numerical factors) to choose a characteristic thickness. The above definition is $2a_I \equiv |d\phi_A/dx|^{-1}$ evaluated at $x = 0$.[1] Physically this is the thickness of a wedge-shaped profile with the slope equal to that of the true profile at $x = 0$. Another definition is a measure of the overlap between the phases:

$$a_L = 2\int_{-\infty}^{\infty} dx\, \phi_A(x)\, \phi_B(x) \qquad (3.4)$$

The factor of 2 has been included so that $a_L = a_I$ for the A/B interface. The measure a_L will be useful for the A/BC interface.

IV. Theory of Polymer Interfaces

(Readers interested primarily in seeing how and why the properties of the polymer interface vary with the parameters may omit this section. It deals with the equations used for the calculation of the interfacial properties.)

In the development of the theory[1-3] interest focuses on quantities $q_K(x)$, which are proportional to the probability density that a very long (essentially infinite) chain, of species K, will have one of its ends at the level x. A middle monomer of a long chain can be viewed as the origin of two such long chains, so the volume fraction of K at x is given by

$$\phi_K(x) = [q_K(x)]^2 \qquad (4.1)$$

The quantities q_K are determined by a modified diffusion equation (as might be expected from the relation of polymer statistics to random walks). The diffusion-like equation must be enhanced to take into account the interactions among the species and also to ensure that the molecules assemble themselves in such a way that the density at any point is a constant (assuming, as we will, that there is zero volume change on mixing).

A. Review of the A/B Interface Theory. For the A/B interface the appropriate equations for q_A and q_B are

$$\frac{b^2}{6}\frac{d^2 q_A(x)}{dx^2} - [\chi_{AB} q_B^2(x) + w(x)]q_A(x) = 0 \qquad (4.2)$$

$$\frac{b^2}{6}\frac{d^2 q_B(x)}{dx^2} - [\chi_{AB} q_A^2(x) + w(x)]q_B(x) = 0 \qquad (4.3)$$

The function $w(x)$ must be chosen in such a way that for all x

$$\phi_A(x) + \phi_B(x) = q_A^2(x) + q_B^2(x) = 1 \qquad (4.4)$$

There are several equivalent formulas for the interfacial tension. One of them is

$$\gamma/\rho_0 k_B T = 2\int_{-\infty}^{\infty} dx\, \chi_{AB}\phi_A(x)\, \phi_B(x) \qquad (4.5)$$

Using eqs 4.2 and 4.3 one can derive the alternative expression

$$\frac{\gamma}{2\rho_0 k_B T} = \int_{-\infty}^{\infty} dx\, \frac{1}{2}\left\{\frac{b^2}{6}\left[\left(\frac{dq_A}{dx}\right)^2 + \left(\frac{dq_B}{dx}\right)^2\right] + \chi_{AB} q_A^2(x)\, q_B^2(x)\right\} \qquad (4.6)$$

The right-hand side of eq 4.6 may be regarded as the action of a classical particle moving in two-dimensions with spatial coordinates q_A and q_B and with x playing the role of time. The motion takes place under the constraint of eq 4.4; i.e., it is confined to a circle. Equations 4.2 and 4.3 are the corresponding Euler–Lagrange equations. Equation 4.5 follows from conservation of "energy", the value of the energy being zero. This analogy to classical mechanics problems is familiar in the theory of solitons and fronts, and it is very helpful for the A/BC interface, too. For the interface problem, the minimization of the "action" is nothing more than the statement that the density profile, as determined by the q_K functions, minimizes the interfacial free energy (i.e., interfacial tension).

There are independent physical derivations of eqs 4.5 and 4.6. Equation 4.5 follows from an argument based on integration of surface energy over a coupling parameter that can be used to put the interface together.[1]

Equation 4.6 can be shown to be the sum of polymer conformational entropy associated with the requirement that the polymer walks turn back into their own phase and a surface energy term arising from the overlap of A and B at the interface.

B. Theory of the A/BC Interface. A simple way of extending the theory of the A/B interface to that of A/BC is via an equation like eq 4.6 for the interfacial tension. Anticipating the usefulness of an analogy to mechanics, we employ a notation paralleling that field; viz., we introduce Lagrangian-, kinetic energy-, and potential energy-like quantities, related by $L = K - V$. Keep in mind that x is a time-like variable.

$$\gamma/\rho_0 k_B T = 2\int_{-\infty}^{\infty} dx\, (K(x) - V(x)) \tag{4.7}$$

$$K(x) = \frac{1}{2}\frac{b^2}{6}\left[\left(\frac{dq_A}{dx}\right)^2 + \left(\frac{dq_B}{dx}\right)^2 + \left(\frac{dq_C}{dx}\right)^2\right] \tag{4.8}$$

$$V(x) = -(1/2)\{\chi_{AB}q_A^2(x)\, q_B^2(x) + \chi_{AC}q_A^2(x)\, q_C^2(x) + \chi_{BC}q_B^2(x)\, q_C^2(x) - q_B^2(x)\Delta\mu_B - q_C^2(x)\Delta\mu_C\} \tag{4.9}$$

The last two terms of υ, with the $\Delta\mu$'s given by eqs 2.2 and 2.3, are needed to remove the bulk free energy from the expression, leaving interfacial tension. The $q_K(x)$'s are determined by functionally minimizing γ with respect to the q_K's but subject to the condition that

$$q_A^2(x) + q_B^2(x) + q_C^2(x) = 1 \tag{4.10}$$

for all x. Minimization yields the equations

$$\frac{b^2}{6}\frac{d^2q_A}{dx^2} - [\chi_{AB}q_B^2(x) + \chi_{AC}q_C^2(x) + w(x)]q_A(x) = 0 \tag{4.11}$$

$$\frac{b^2}{6}\frac{d^2q_B}{dx^2} - \{\chi_{AB}q_A^2(x) + \chi_{BC}[q_C^2(x) - \phi_{C\infty}^2] + w(x)\}q_B(x) = 0 \tag{4.12}$$

$$\frac{b^2}{6}\frac{d^2q_C}{dx^2} - \{\chi_{AC}q_A^2(x) + \chi_{BC}[q_B^2(x) - \phi_{B\infty}^2] + w(x)\}q_C(x) = 0 \tag{4.13}$$

where $w(x)$ is a function that must be chosen such that eq 4.10 is satisfied for all x.

There is actually an easier way to proceed, an extension of the method used for the A/B interface.[1] Rather than drawing the analogy to a constrained three-dimensional motion in a space with "coordinates" q_A, q_B, and q_C (instead of x, y, z), one can confine the motion to the unit sphere, as required by eq 4.10, by writing

$$q_A = \cos\theta$$

$$q_B = \sin\theta\cos\phi$$

$$q_C = \sin\theta\sin\phi \tag{4.14}$$

and regarding $\theta(x)$ and $\phi(x)$ as the dependent variables. Then no constraint condition, hence no $w(x)$ function, enters. (There should be no confusion between the angle, ϕ, which is never subscripted with a letter, and volume fraction variables, which are always subscripted with a letter.)

The mechanics problem analogous to the A/BC interface problem can now be put as follows. We need to know about the motion of a "particle" that falls off the pole of a sphere at a time (variable x) infinitely in the past, moves through a potential

$$V = -\frac{1}{2}\{\cos^2\theta\sin^2\theta(\chi_{AB}\cos^2\phi + \chi_{AC}\sin^2\phi) + \chi_{BC}\sin^2\theta[\sin^2\theta\cos^2\phi\sin^2\phi - (\cos^2\phi\sin^4\alpha + \sin^2\phi\cos^4\alpha)]\} \tag{4.15}$$

with potential energy

$$K = \frac{1}{2}\left[\left(\frac{d\theta}{dx}\right)^2 + \sin^2\theta\left(\frac{d\phi}{dx}\right)^2\right] \tag{4.16}$$

and arrives at the equator, with longitudinal angle α, at a time of $+\infty$. The angle α is defined such that $\cos^2\alpha = \phi_{B\infty}$.

To be quantitative it is convenient to go over to a Hamiltonian formulation of the equations of motion, introducing the conjugate momenta to θ and ϕ. This yields

$$\frac{d\theta}{dx} = \frac{6}{b^2}p_\theta \tag{4.17}$$

$$\frac{d\phi}{dx} = \frac{6}{b^2}\frac{p_\phi}{\sin^2\theta} \tag{4.18}$$

$$\frac{dp_\theta}{dx} = \cos\theta\sin\theta(\cos^2\theta - \sin^2\theta)(\chi_{AB}\cos^2\phi + \chi_{AC}\sin^2\phi) + \chi_{BC}\cos\theta\sin\theta[2\sin^2\theta\cos^2\phi\sin^2\phi - (\cos^2\phi\sin^4\alpha + \sin^2\phi\cos^4\alpha)] + \frac{b^2}{6}\frac{\cos\theta}{\sin^3\theta}p_\phi^{\ 2} \tag{4.19}$$

$$\frac{dp_\phi}{dx} = \sin^2\theta\cos\phi\sin\phi\{(\chi_{AC} - \chi_{AB})\cos^2\theta + \chi_{BC}[(\sin^2\theta(\cos^2\phi - \sin^2\phi) + (\sin^4\alpha - \cos^4\alpha)]\} \tag{4.20}$$

The conserved energy for this problem is $K(x) + V(x) = 0$.

Once one has the interfacial concentration profiles, one could use eq 4.7 to calculate the interfacial tension. The equivalent expressions

$$\gamma/\rho_0 k_B T = -4\int_{-\infty}^{\infty} dx\ V(x) \tag{4.21}$$

$$= 4\int_{-\infty}^{\infty} dx\ K(x) \tag{4.22}$$

are more convenient.

Some details of the numerical solution for the trajectory are presented in Appendix A. It is a bit tricky since the initial and final points are unstable fixed points of the equations.

V. Distribution of the B and C Polymers Well into the A Phase

Usually, as one gets away from the interfacial region and well into the A phase (large negative x), either polymer B or C will dominate; i.e., the ratio of B to C concentration will go to either infinity or zero. In this section we will discuss this matter, presenting a physical derivation of the criterion for deciding which dominates. In Appendix A we will get more quantitative. In section VI.A we will discuss the case where the ratio of B to C remains everywhere constant.

Consider that we are at a point x fairly deep into the A phase, where both B and C are present to some extent, but they are quite dilute. Consider what the free energy change, per monomer, would be if we changed one of the B chains there into a chain of C. We do it as follows. Take a monomer of B away from x, for a free energy change (in units of k_BT) of $-\chi_{AB}$. Put it into the mixed phase (at $x = \infty$), for a free energy change of $\Delta\mu_B$. Take a monomer of C from the mixed phase, for a free energy change of $-\Delta\mu_C$. Put it at x for a free energy change of χ_{AC}. (Forget about the breaking of the chain, since we are going to eventually do this repeatedly enough to reconstruct a chain.) If the cost of the operation is positive

$$\chi_{AC} - \Delta\mu_C - \chi_{AB} + \Delta\mu_B = \chi_{AC} - \chi_{AB} - \chi_{BC}(\phi_{B\infty} - \phi_{C\infty}) > 0 \quad (5.1)$$

(we have used $\phi_{B\infty}^2 - \phi_{C\infty}^2 = \phi_{B\infty} - \phi_{C\infty}$), then the process does not spontaneously occur. This means that B is the dominant polymer well into the A half-space. If the sign of the inequality 5.1 is the other way, then C is dominant. In Appendix A it will be shown that the ratio of the C to the B polymer concentration falls off as

$$\exp\{[(\chi_{AC} - \chi_{BC}\phi_{B\infty}^2)^{1/2} - (\chi_{AB} - \chi_{BC}\phi_{C\infty}^2)^{1/2}]x\}$$

as $x \to -\infty$. This will fall to zero if inequality 5.1 is satisfied.

We have adopted the convention throughout this paper, except where noted, that B is the component that dominates in the A region; i.e., B and C are named such that inequality 5.1 is satisfied.

VI. Limiting Cases

A. The Ratio of B to C Stays Constant. The situation where (5.1) is an equality

$$\chi_{AC} - \chi_{AB} - \chi_{BC}(\phi_{B\infty} - \phi_{C\infty}) = 0 \quad (6.1)$$

is an interesting one to address and one that will be important in our later discussion of the results of calculations. In this case we show in Appendix B that the ratio of the concentrations of B to C remains constant throughout and the interfacial properties can be found analytically. They correspond to that of, what we might call, an A/B′ interface with an effective χ parameter, χ', given by

$$\chi' = \chi_{AB}\phi_{B\infty} + \chi_{AC}\phi_{C\infty} + |\chi_{BC}|\phi_{B\infty}\phi_{C\infty} \quad (6.2)$$

The A concentration is given by eq 3.2 with χ' replacing χ_{AB}. The B′ concentration is then given by eq 3.3 and is divided into B and C so that the ratio of B to C remains $\phi_{B\infty}/\phi_{C\infty}$ for all x. The interfacial tension is $\gamma = 6^{-1/2}k_BT\rho_0 b(\chi')^{1/2}$, and the overlap is $a_L = b/(6\chi')^{1/2}$. Of course, there is no adsorption of B to the interface.

B. When C is Strongly Excluded from Overlap with A. In Figure 1 we see the concentration profile of an interface for which $\chi_{AC}/\chi_{AB} = 8$, $\chi_{BC}/\chi_{AB} = -0.25$, and $\phi_{B\infty} = 0.5$. Note that there is little overlap between C and A under these conditions. When this is the case there are some properties of the interface that can be obtained analytically. Let us divide the interfacial region into two parts. The first, called region I, will be on the left, where the A concentration falls from a value of unity to a very small value and the B concentration builds up to a value close to unity. Finally, when the A concentration has decreased significantly, the C concentration can start to build up; and this region on the right, starting at some $x > 0$, we shall label II.

Let us first estimate where the break between regions I and II occurs. The x corresponding to the maximum of $\phi_{B\infty}(x)$ might be ideal, but it is hard to locate via some closed-formed expression (without solving the differential equations). Therefore, we will select another point, which should be close-by. Consider that we are at some position x where the concentrations of A and C are small and $\phi_B \approx 1$. We want to know if we are far enough out to start building up the concentration of C while bringing the concentration of B back down toward $\phi_{B\infty}$. The cost of having one less monomer of B at that level and one more monomer of C is an increase $(\chi_{AC} - \chi_{AB})\phi_A$ in free energy due to interactions with A. However, the free energy decreases by $\chi_{BC}(\phi_B - \phi_C)$ by virtue of an increase in the number of BC interactions. There is also a change in the free energy (the osmotic term) of $\Delta\mu_B - \Delta\mu_C = \chi_{BC}(\phi_{C\infty} - \phi_{B\infty})$ due to the fact that the C monomer has to be taken out of the bulk and replaced by the B. Thus, when $\phi_A(x)$ has fallen to such a low value that

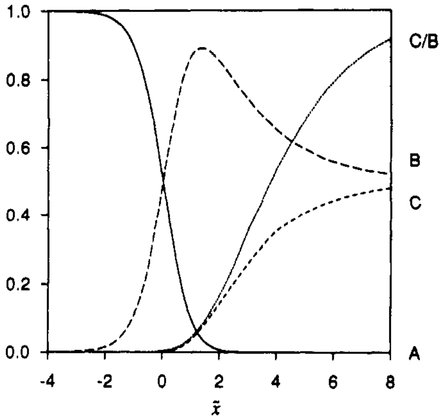

Figure 1. Concentration profile for an A/BC interface with $\tilde{\chi}_{AC} = 8$, $\tilde{\chi}_{BC} = -0.25$, and $\phi_{B\infty} = 0.5$. The solid line is the profile (volume fraction) of A, the long dashes the profile of B, and the short dashes the profile of C. The dotted line is the ratio $[\phi_C(x)/\phi_B(x)][\phi_{B\infty}/\phi_{C\infty}]$.

$$(\chi_{AC} - \chi_{AB})\phi_A - |\chi_{BC}|(\phi_B - \phi_C + \phi_{C\infty} - \phi_{B\infty}) = 0 \quad (6.3)$$

one has reached a point where it pays to start building up the C concentration. (Comparison with eq 4.20 reveals that this is also where $dp_\phi/dx = 0$.) If there is to be a good separation of regions, then $\phi_A(x)$ should be small at this point. This requires that $\chi_{AC} - \chi_{AB}$ be large, or $|\chi_{BC}|$ be small, or $\phi_{B\infty}$ be close to unity. When ϕ_A is small near the I–II boundary, its value, call it $\phi_{A,0}$, can be approximated as

$$\phi_{A,0} = 2|\chi_{BC}|(1 - \phi_{B\infty})/(\chi_{AC} - \chi_{AB}) \quad (6.4)$$

In Appendix C we derive expressions for the concentration profiles that are valid everywhere except near the boundary between regions I and II. The important physics to note is that in region I, although essentially no C is present, the interface is not exactly like an A/B interface. That is because in addition to the A–B interactions acting on B units, there is an osmotic force arising from the chemical potential terms. This osmotic force tends to remove B polymer from regions where component C is not present or is present at concentration less than $\phi_{B\infty}$. In Appendix C approximate expressions, including estimates that go beyond the asymptotic limit, are given for the overlap length, a_L, and the interfacial tension, γ. The expression for γ is not as good as one might like because important contributions, coming from the zone near the I–II boundary, are omitted.

VII. Properties of the A/BC Interface As the Parameters Are Varied

The independent parameters that have been introduced in the present model of the A/BC interface are b, ρ_0, χ_{AB},

χ_{AC}, χ_{BC}, and $\phi_{B\infty}$. The first three can be considered as scaling the physical properties of the system. This is analogous to the way they scale the properties of the A/B interface. Thus, one may define the reduced interfacial tension

$$\tilde{\gamma} = \frac{\gamma}{6^{-1/2} k_B T \rho_0 b \chi_{AB}^{1/2}} \tag{7.1}$$

reduced distance

$$\tilde{x} = \frac{x}{b(6\chi_{AB})^{-1/2}} \tag{7.2}$$

(similarly for $\tilde{a}_L$), and reduced χ parameters

$$\tilde{\chi}_{KL} = \chi_{KL}/\chi_{AB} \tag{7.3}$$

(Sometimes we will explicitly write $\tilde{\chi}_{AB}$, even though it equals unity, in order to make the physical dependencies clearer.) A reduced measure of the excess B adsorbed to the surface is

$$\tilde{n}_{xsB} = \frac{n_{xsB}}{6^{-1/2}\rho_0 b} \tag{7.4}$$

Except for these multiplicative scaling factors, the properties of the system depend on three parameters: $\tilde{\chi}_{AC}$, $\tilde{\chi}_{BC}$, and $\phi_{B\infty}$. In this section we will report the theoretical predictions of how the properties vary as these parameters are varied. We will also describe physically why the variations observed occur. Results for a wide variety of parameter values are summarized in Table I. (Not all the points shown in the figures are included in the table.)

To begin let us look in some depth at a system with a particular set of parameters that will serve as a benchmark: $\tilde{\chi}_{AC} = 2$, $\tilde{\chi}_{BC} = -0.25$, and $\phi_{B\infty} = 0.5$. Figure 2 shows the concentration profiles across the interface for this system. The most striking feature is how rapidly the ratio of C to B concentration (dotted curve) falls to zero as one goes from the blend phase toward the A region. The falloff is rapid even in the region where hardly any A is present. Even though the sum of B and C concentration is falling as one moves from right to left, the B concentration actually has a region in which it rises. By the time one reaches the positions near $\tilde{x} = 0$, where there are significant amounts of A, there is little C present. The interfacial tension calculated for this case is $\tilde{\gamma} = 1.167$, the overlap is $\tilde{a}_L = 0.906$, and the excess B is $\tilde{n}_{xsB} = 0.857$.

The effect of component B dominating the interface is even more striking as one increases the value of $\tilde{\chi}_{AC}$. We see that in the concentration profiles of Figure 1, where $\tilde{\chi}_{BC} = -0.25$ and $\phi_{B\infty} = 0.5$ again, but now $\tilde{\chi}_{AC} = 8$. This is a case where the regions I and II of section VI.B are well defined. At the boundary, ϕ_{A0}, given by eq 6.4, has the very small value of 0.036. (This occurs at $\tilde{x} = 1.41$. The maximum in ϕ_B occurs at $\tilde{x} = 1.36$, where $\phi_A = 0.040$.) The interfacial tension in this case is $\gamma = 1.278$. This may be compared with the estimate 1.216 for the well separated A and C, according to eqs C.7 plus C.13. As stated earlier, one cannot expect great accuracy away from the asymptotic limit. Note that γ differs considerably from simply the value of an A/B interface, which would be 1. The overlap is $\tilde{a}_L = 0.916$. Equation C.8 predicts a value of 0.874, which is only moderately good. The excess B is $\tilde{n}_{xsB} = 1.709$. Equation C.9 plus eq C.14 predicts 1.910, the considerable error being a reflection of the importance of the I–II boundary region.

In general the repulsion between A and C is driving the C component away from the interface and filling the space with B. However, this separation of B from C costs free energy, since the interaction parameter χ_{BC} is negative (attractive). To illustrate the effect of increasing $\tilde{\chi}_{BC}$ look at the case where $\tilde{\chi}_{AC} = 2$ and $\phi_{B\infty} = 0.5$, but $\tilde{\chi}_{BC} = -2$ (compared with the benchmark, which has $\tilde{\chi}_{BC} = -0.25$). The profiles are shown in Figure 3. In contrast with Figure 2, much less repulsion of the C has occurred, although the value of χ_{AC} is the same. The repulsion has been suppressed by the large energy needed to separate B from C. Neither of the limits discussed in section VI pertain.

Table I
Properties Calculated for Several Values of the Parameters

$\tilde{\chi}_{AC}$	$\tilde{\chi}_{BC}$	$\phi_{B\infty}$	$\tilde{\gamma}$	$\tilde{a}_L$	$\tilde{n}_{xsB}$
2	−0.25	0.5	1.1670	0.8567	0.9063
1.05	−0.25	0.5	1.0425	0.0611	0.9596
1.1	−0.25	0.5	1.0535	0.1202	0.9505
1.2	−0.25	0.5	1.0733	0.2326	0.9361
1.5	−0.25	0.5	1.1193	0.5204	0.9137
2.5	−0.25	0.5	1.1954	1.0729	0.9080
5	−0.25	0.5	1.2522	1.5227	0.9144
6	−0.25	0.5	1.2632	1.6024	0.9154
8	−0.25	0.5	1.2776	1.7085	0.9156
1.5	−0.25	0.05	1.2152	0.3149	0.8272
1.75	−0.25	0.05	1.2963	0.6344	0.7877
2	−0.25	0.05	1.3648	0.8886	0.7689
1.05	−0.1	0.5	1.0242	0.1426	0.9769
1.25	−0.1	0.5	1.0608	0.6586	0.9530
1.5	−0.1	0.5	1.0898	1.1344	0.9461
2	−0.1	0.5	1.1199	1.6962	0.9499
5	−0.1	0.5	1.1677	2.4968	0.9657
5	−0.2	0.5	1.2264	1.7250	0.9282
5	−0.5	0.5	1.3493	1.0077	0.8576
5	−1	0.5	1.4755	0.6330	0.7785
5	−2	0.5	1.6372	0.3710	0.6823
2	−0.2	0.5	1.1543	1.0194	0.9186
2	−0.5	0.5	1.2140	0.4890	0.8614
2	−1	0.5	1.2813	0.2683	0.8050
2	−2	0.5	1.3881	0.1406	0.7338
2	−0.25	0.1	1.3407	0.8736	0.7835
2	−0.25	0.25	1.2755	0.8699	0.8302
2	−0.25	0.75	1.0661	0.7279	0.9705
2	−0.25	0.9	1.0182	0.5201	0.9945
2	−0.5	0.1	1.3795	0.3188	0.7363
2	−0.5	0.25	1.3259	0.3952	0.7764
2	−0.5	0.5	1.2140	0.4890	0.8614
2	−0.5	0.75	1.0864	0.4753	0.9481
2	−0.5	0.9	1.0254	0.3598	0.9903
1.5	−0.25	0.02	1.2207	0.3043	0.8234
1.5	−0.25	0.1	1.2070	0.3397	0.8345
1.5	−0.25	0.75	1.0524	0.5282	0.9692
1.1	−0.5	0.5	1.0831	0.0636	0.9241
1.5	−0.5	0.5	1.1541	0.2828	0.8804
1.5	−2	0.4	1.3339	0.0152	0.7499

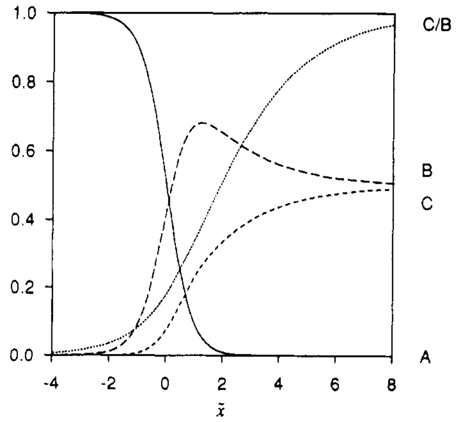

Figure 2. Concentration profile with $\tilde{\chi}_{AC} = 2$, $\tilde{\chi}_{BC} = -0.25$, and $\phi_{B\infty} = 0.5$. The solid line is the profile (volume fraction) of A, the long dashes the profile of B, and the short dashes the profile of C. The dotted line is the ratio $[\phi_C(x)/\phi_B(x)][\phi_{B\infty}/\phi_{C\infty}]$.

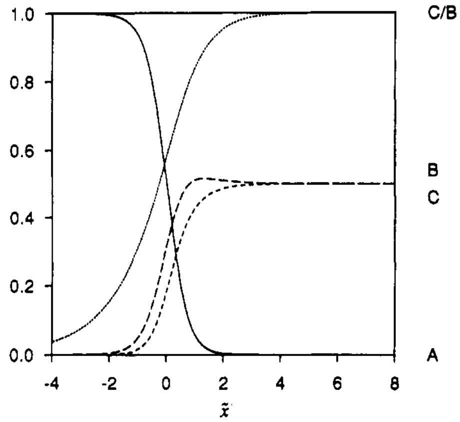

Figure 3. Concentration profile with $\tilde{\chi}_{AC} = 2$, $\tilde{\chi}_{BC} = -2$, and $\phi_{B\infty} = 0.5$. See caption to Figure 2 for legend.

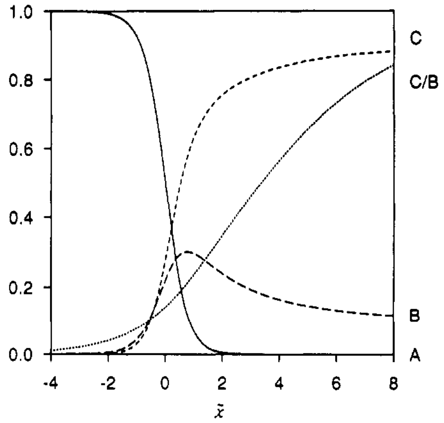

Figure 4. Concentration profile with $\tilde{\chi}_{AC} = 2$, $\tilde{\chi}_{BC} = -0.25$, and $\phi_{B\infty} = 0.1$. See caption to Figure 2 for legend.

Calculated values of the physical parameters can be found in Table I.

Figure 4 illustrates how a fairly small amount of B can greatly modify the properties of the interface. One sees that, although the ratio of ϕ_C to ϕ_B in the mixed phase is 9:1, the two components have roughly equal concentration in the region of significant overlap with A. We also see how spread out the approach of ϕ_C and ϕ_B to the equilibrium concentrations can be. It goes (cf. Appendix A) with a characteristic reduced distance scale of $(4|\tilde{\chi}_{BC}|\phi_{B\infty}\phi_{C\infty})^{-1/2}$, which is 3.333 for these parameters. The interfacial tension in this case is $\tilde{\gamma} = 1.342$, which might be compared with a binary A/C reduced interfacial tension of 1.414. It is interesting to also make a comparison with the reduced interfacial tension of a hypothetical interface where the ratio of C to B remains constant, which would be $(\tilde{\chi}')^{1/2} = 1.387$.

Next, let us examine a case approaching the conditions under which the ratio of ϕ_C/ϕ_B would remain constant, as discussed in section VI.A. Consider the system with parameters $\tilde{\chi}_{AC} = 1.5$, $\tilde{\chi}_{BC} = -2$, and $\phi_{B\infty} = 0.4$. The combination $\chi_{AC} - \tilde{\chi}_{AB} - \chi_{BC}(\phi_{B\infty} - \phi_{C\infty}) = 0.1$ is close to the zero value that would lead to the properties being like an A/B interface with effective χ parameter

$$\tilde{\chi}' = \tilde{\chi}_{AB}\phi_{B\infty} + \tilde{\chi}_{AC}\phi_{C\infty} + |\tilde{\chi}_{BC}|\phi_{B\infty}\phi_{C\infty} = 1.78$$

In Figure 5 we see indeed that the ratio of C to B does not fall off significantly until values of x well inside the A phase. The calculated interfacial tension is $\tilde{\gamma} = 1.3339$, to be compared with $(\tilde{\chi}')^{1/2} = 1.3342$. The overlap is $\tilde{a}_L = 0.74986$ compared with $(\tilde{\chi}')^{-1/2} = 0.74953$. The adsorption is $\tilde{n}_{xsB} = 0.0152$, small, but not quite zero.

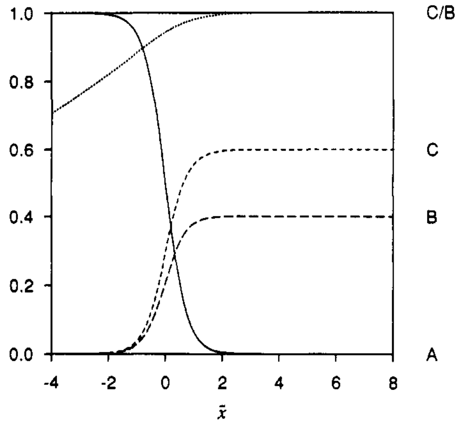

Figure 5. Concentration profile with $\tilde{\chi}_{AC} = 1.5$, $\tilde{\chi}_{BC} = -2$, and $\phi_{B\infty} = 0.4$. See caption to Figure 2 for legend.

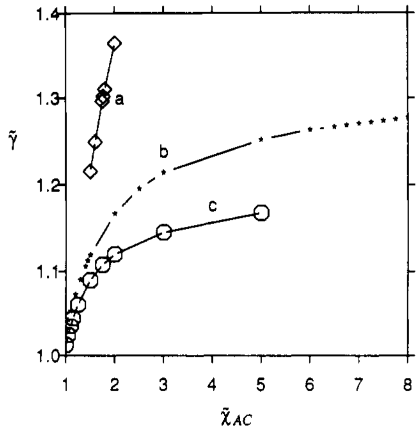

Figure 6. Variation of interfacial tension with $\tilde{\chi}_{AC}$. (a) $\tilde{\chi}_{BC} = -0.25$, $\phi_{B\infty} = 0.05$; (b) $\chi_{BC} = -0.25$, $\phi_{B\infty} = 0.5$; (c) $\chi_{BC} = -0.1$, $\phi_{B\infty} = 0.5$. The properties were determined at the marked points. The lines are meant only to guide the eye.

With the results for $\tilde{\chi}_{AC} = 2$, $\tilde{\chi}_{BC} = -0.25$, and $\phi_{B\infty} = 0.5$ as a benchmark, let us consider the effect on the interfacial tension and overlap of varying one or two parameters at a time. In all the following figures the stars represent the result of varying only one of the parameters, while the diamonds and octagons show the effects of changing two parameters. We begin by varying the interaction parameter $\tilde{\chi}_{AC}$. This drives the C component away from overlap with A. The resulting reduced interfacial tension is plotted in Figure 6 for three different sets of values of the other parameters, $\tilde{\chi}_{BC}$ and $\phi_{B\infty}$. As would be expected the interfacial tension goes up with increased $\tilde{\chi}_{AC}$, but eventually it levels off when the C polymer is largely excluded from overlap with A. The asymptotic limit of eqs C.7 and C.13 is independent of $\tilde{\chi}_{AC}$. Curve b should level off to a value of 1.412. Curve c shows that when $\tilde{\chi}_{BC}$ is decreased it is easier to pull the B component away from C and into the region of A overlap. Hence the interfacial tension is lower, and it is predicted that it will level off to 1.234. Curve a shows the effect of having only a small amount of B present. There is not enough B to keep the value of $\tilde{\gamma}$ much below $\tilde{\chi}_{AC}^{1/2}$. Considering that there is only a 0.05 volume fraction of B in the mixed phase, the interfacial tension is lowered quite a bit. For instance, consider the point on curve a corresponding to $\tilde{\chi}_{AC} = 2$. The calculated value of $\tilde{\gamma}$ is 1.363, which may be compared with $\tilde{\chi}_{AC}^{1/2} = 1.414$ or $(\tilde{\chi}')^{1/2} = 1.401$. Remember that even an A/B interface would have $\tilde{\gamma} = 1$. Thus this 5% B reduces the interfacial tension 12.4% from the A/C toward the A/B value.

Figure 7 shows the measure of overlap, $\tilde{a}_L$. Curve b

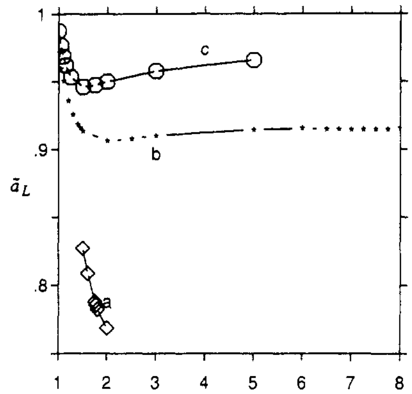

Figure 7. Variation of overlap distance with $\tilde{\chi}_{AC}$. See caption to Figure 6 for legend.

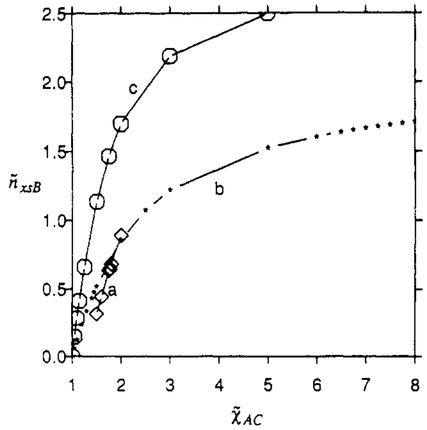

Figure 8. Variation of excess B in the interface with $\tilde{\chi}_{AC}$. See caption to Figure 6 for legend.

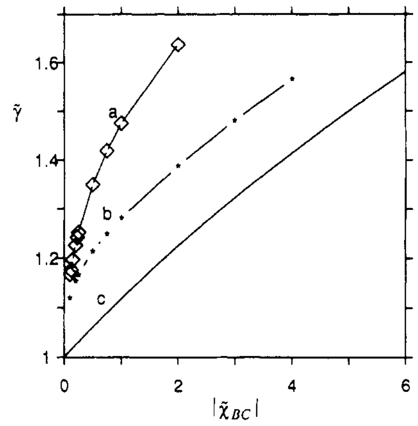

Figure 9. Variation of interfacial tension with $\tilde{\chi}_{BC}$. All curves have $\phi_{B\infty} = 0.5$. (a) $\tilde{\chi}_{AC} = 5$; (b) $\tilde{\chi}_{AC} = 2$; (c) $\tilde{\chi}_{AC} = 1$ (exact, based on $\tilde{\chi}'$).

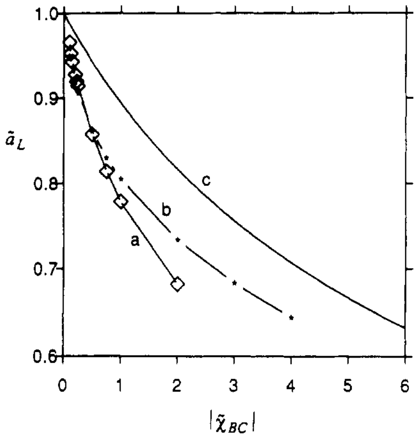

Figure 10. Variation of overlap distance with $\tilde{\chi}_{BC}$. See caption to Figure 9 for legend.

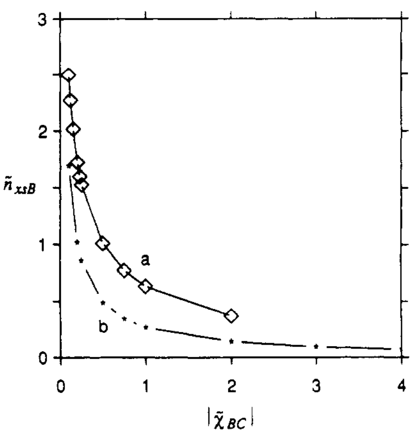

Figure 11. Variation of excess B in the interface with $\tilde{\chi}_{BC}$. All curves have $\phi_{B\infty} = 0.5$. (a) $\tilde{\chi}_{AC} = 5$; (b) $\tilde{\chi}_{AC} = 2$. For $\tilde{\chi}_{AC} = 1$ and $\phi_{B\infty} = 0.5$ there is no adsorption.

starts at $\tilde{a}_L = 0.970$, the exact value given by $(\tilde{\chi}')^{-1/2}$. The overlap drops as the repulsion from C becomes greater. Then $\tilde{a}_L$ goes through a minimum as a function $\tilde{\chi}_{AC}$. Finally, it approaches the asymptotic limit of eq C.8, which is 0.900. However, for $\chi_{AC} = 8$ we calculate $\tilde{a}_L = 0.916$. The approach to the asymptotic value appears to be from above. The prediction of Appendix C is that it would be from below. Hence for overlap the proposed method of backing away from the asymptote has room for improvement. (One probably has to account for the overlap of A with C. We see no way that the true asymptotic limit for $\tilde{a}_L$ can be wrong.)

Figure 8 shows the adsorption of B to the interface. For large $\tilde{\chi}_{AC}$ one expects the excess B to level off at some value, and the curves appear to do so. Perhaps the most surprising of the curves is curve a, where $\phi_{B\infty} = 0.05$. There is a very large amount of adsorption, eventually exceeding the amount adsorbed when $\phi_{B\infty} = 0.5$. We will have more to say about the behavior at low B concentration below.

Now let us look at $\tilde{\gamma}$, $\tilde{a}_L$, and $\tilde{n}_{xsB}$ from the point of view of varying $\tilde{\chi}_{BC}$, with the other two parameters held constant. In Figures 9 and 10 we show the result of varying $\tilde{\chi}_{BC}$ with $\tilde{\chi}_{AC} = 5$, 2, and 1 and $\phi_{B\infty} = 0.5$. When $\tilde{\chi}_{BC}$ is large, components B and C find it difficult to separate, so the approximation discussed in section VI.A becomes exact. In fact for $\tilde{\chi}_{AC} = 1$ and $\phi_{B\infty} = 0.5$ the system behaves like an A/B′ interface for all negative χ_{BC}. Thus the solid curves c in the figures are the exact results of using $\tilde{\chi}' = 1 + (1/4)\tilde{\chi}_{BC}$, and $\tilde{\gamma} = (\tilde{\chi}')^{1/2}$ and $\tilde{a}_L = (\tilde{\chi}')^{-1/2}$.

When $|\chi_{BC}|$ is small it is very easy to have B replace C in the region where A is present. Furthermore, once the B has built up, and when the A concentration becomes very small, there is a long characteristic distance for return of the B concentration to $\phi_{B\infty}$. This relaxation distance is $2(\phi_{B\infty}\phi_{C\infty}|\tilde{\chi}_{BC}|)^{1/2}$, in reduced units. The interfacial tension of the region where B returns to concentration $\phi_{B\infty}$ approaches zero like $|\chi_{BC}|^{1/2}$, so the total reduced interfacial tension approaches unity like $|\tilde{\chi}_{BC}|^{1/2}$.

The adsorption of B is most directly observed in Figure 11, which gives the values of $\tilde{n}_{xsB}$ vs $|\tilde{\chi}_{BC}|$. One should note that implicit in Figure 11 is another curve; viz., when $\tilde{\chi}_{AC} = 1$ and $\phi_{B\infty} = 0.5$, then $\tilde{n}_{xsB} = 0$, as discussed in section VI.A.

Finally, let us consider the effect of varying the concentration $\phi_{B\infty}$, as illustrated in Figures 12 and 13. For $\phi_{B\infty} = 0$ the curves are anchored at the values for an A/C interface, $\tilde{\gamma} = \tilde{\chi}_{AC}^{1/2}$ and $\tilde{a}_L = \tilde{\chi}_{AC}^{-1/2}$. For $\phi_{B\infty} = 1$ all the

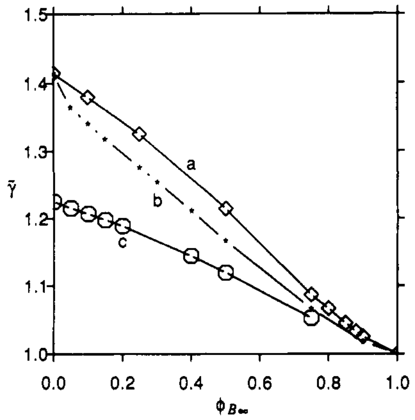

Figure 12. Variation of interfacial tension with $\phi_{B\infty}$. (a) $\tilde{\chi}_{AC}$ = 2, $\tilde{\chi}_{BC}$ = −0.5; (b) $\tilde{\chi}_{AC}$ = 2, $\tilde{\chi}_{BC}$ = −0.25; (c) $\tilde{\chi}_{AC}$ = 1.5, $\tilde{\chi}_{BC}$ = −0.25.

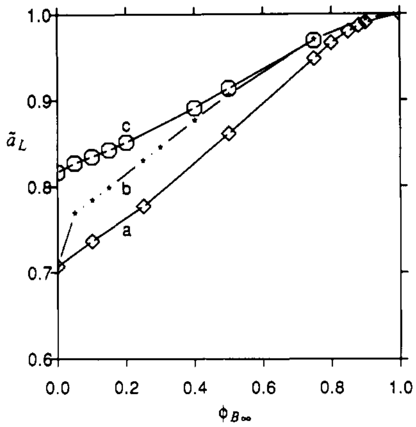

Figure 13. Variation of overlap distance with $\phi_{B\infty}$. See caption to Figure 12 for legend.

curves go to unity. Perhaps the most interesting aspect of the figures is the rapid decrease of the interfacial tension and the rapid rise of the overlap with the first addition of polymer B. This is not so surprising in view of the following fact about the case where $\phi_{B\infty}$ = 0.02, $\tilde{\chi}_{AC}$ = 2, and $\tilde{\chi}_{BC}$ = −0.25. By the time one gets to the point $\tilde{x}$ = 0, where ϕ_A is very close to 0.5, the ratio of C to B concentration is 2.25:1, not 49:1 as in the bulk. Thus even for such small amounts of B, a perturbation theory would not be very accurate. (Before discussing further the behavior near small concentrations of B, we should inject a note of caution. Our computer programs appear to be having some difficulty handling the small $\phi_{B\infty}$ case, and we are not sure that the accuracy in the third or fourth decimal is sufficient to affirm some of the more subtle conclusions we are about to discuss. The way to proceed is to do perturbation theory on the A/C interface. Such a perturbation theory is singular, with difficulties developing at both large negative and positive $\tilde{x}$. We plan to do such a perturbation theory in the future.) Looking at curves c of Figures 12 and 13, one sees that if one weakens the A–C repulsion down to $\tilde{\chi}_{AC}$ = 1.5, there is much less adsorption of B, and the sharp change near the $\phi_{B\infty} \rightarrow 0$ limit is not prominent. For $\phi_{B\infty}$ = 0.02 the ratio of C to B at $\tilde{x}$ = 0 is still a fairly large 10.8:1. Likewise, if one increases the B–C attraction to $\tilde{\chi}_{BC}$ = −0.5, as in curves a, the B and C components find it more difficult to separate, so there is much less adsorption, and less sharp a change with small added B.

The concentration dependence of the excess B is interesting. It is shown in Figure 14. For concentrations approaching pure B the excess B goes to zero. However, for $\phi_{B\infty}$ approaching the smallest values we have been able to study, the excess B appears to approach a finite value.

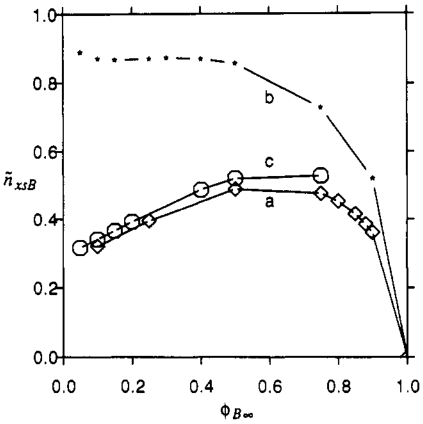

Figure 14. Variation of excess B in the interface with $\phi_{B\infty}$. See caption to Figure 12 for legend.

Examination of the contributions from each half-space reveals that the finite value is coming from the positive $\tilde{x}$ side. It is true that the relaxation distance for component B to go from a value characteristic of the interface to $\phi_{B\infty}$ approaches infinity as $\phi_{B\infty} \rightarrow 0$, but it only does so as $(\phi_{B\infty})^{-1/2}$. That means that for $\tilde{n}_{xsB}$ to stay finite, the concentration of B at typical values of $\tilde{x}$ would have to be of order $(\phi_{B\infty})^{1/2}$, not the first power. This is an issue that is in need of further study by perturbation theory, and by modifying the code to handle small $\phi_{B\infty}$ better.

Other than the region near $\phi_{B\infty}$ = 0, the interfacial tension is fairly linear as a function of concentration for the cases studied. We have not been able to find a method of estimating $\tilde{\gamma}$ that would demonstrate the reasonableness of this near linearity. In arguments we have tried to develop there are positive and negative terms, so it is hard to tell what the sum will be. Frankly, we expected more of an upward bowing, i.e., a more rapid approach to the A/B-like character.

VIII. Summary and Discussion

In this paper we develop the theory of the A/BC interface. By solving the appropriate equations quantitative results are obtained for the concentration profiles, the interfacial tension, a characteristic overlap distance between the A and the BC phase, and the amount of B adsorbed to the interface. The discussion is carried out in terms of parameters reduced by values appropriate to the A/B interface. There are three intrinsically new parameters when component C is present: $\tilde{\chi}_{AC} = \chi_{AC}/\chi_{AB}$, $\tilde{\chi}_{BC} = \chi_{BC}/\chi_{AB}$, and the composition variable for the BC phase, $\phi_{B\infty}$. When the relation $\chi_{AC} - \chi_{AB} - \chi_{BC}(2\phi_{B\infty} - 1) = 0$ then the ratio of B to C remains constant through the interface and the properties may be expressed in closed form in terms of an effective χ parameter. In general, one polymer adsorbs to the interface (we call this one the B polymer). It is this adsorption that modifies the properties, sometimes strongly. The adsorption follows the rules that are well-known for surface-active agents. However, for polymers the adsorption is stronger because their is no entropy of mixing term tending to homogenize, and the interfaces are thicker. Increasing $\tilde{\chi}_{AC}$ repels C from the interfacial region, increasing B adsorption. Increasing $|\tilde{\chi}_{BC}|$ (χ_{BC} is negative) has the opposite effect since it makes it more energetically unfavorable to separate B from C. Even fairly small amounts of B in the BC phase can lead to a considerable adsorption and consequent modification of the interfacial properties.

Acknowledgment. The author would like to thank Prof. Philip Baldwin for his interest and efforts during

the initial stage of this research and especially for some early work on numerical solution of the differential equations.

Appendix A: Numerical Solution of the Differential Equations

In section IV.B a word description of the analogy between the differential equations for the interfacial profiles and the motion of a point on a sphere was given. The differential equations are eqs 4.17–4.20. There are some features of this problem that prevent one from simply using a library program for differential equations. The first is that the boundary conditions are given at the beginning and end of the trajectory. Most programs are for initial conditions given, but there are some for two or more point boundary conditions. The latter also did not prove to be useful because the initial and final points of the trajectory are unstable fixed points, which have to be approached in very special ways. We require that at "time" $\tilde{x} \to -\infty$ the particle roll off the pole with velocity approaching zero. At "time" $\tilde{x} \to \infty$ the particle must come up to the equator ($\theta = \pi/2$) and stop at $\phi = \alpha$. In order for this to happen to particle must start and stop heading in just the right direction, and with just the right momentum–time relation. These asymptotic laws can be determined by an analytic consideration of the linearized equations appropriate near the pole and equator.

For $\tilde{x} \to -\infty$ the analysis is clearer working with the original equations for the $q_K(\tilde{x})$, rather than θ and ϕ. So we return to eqs 4.12 and 4.13 and select the largest terms as $\tilde{x} \to -\infty$. In this case $q_A \sim 1$, while q_B and q_C are small. Also w is small, reflecting the fact that it goes to zero in the bulk A phases. Hence the important parts of eqs 4.12 and 4.13 to consider are

$$\frac{d^2 q_B}{d\tilde{x}^2} = (\tilde{\chi}_{AB} - \tilde{\chi}_{BC}\phi_{C\infty}^2) q_B \qquad (A.1)$$

$$\frac{d^2 q_C}{d\tilde{x}^2} = (\tilde{\chi}_{AC} - \tilde{\chi}_{BC}\phi_{B\infty}^2) q_C \qquad (A.2)$$

The asymptotic solutions are

$$q_B(\tilde{x} \to -\infty) \propto \exp[(\tilde{\chi}_{AB} - \tilde{\chi}_{BC}\phi_{C\infty}^2)^{1/2}\tilde{x}] \qquad (A.3)$$

$$q_C(\tilde{x} \to -\infty) \propto \exp[(\tilde{\chi}_{AC} - \tilde{\chi}_{BC}\phi_{B\infty}^2)^{1/2}\tilde{x}] \qquad (A.4)$$

By means of eqs 4.14 this may be translated into

$$\theta(\tilde{x} \to -\infty) \approx q_B(\tilde{x}) \approx g_1 \exp[(\tilde{\chi}_{AB} - \tilde{\chi}_{BC}\phi_{C\infty}^2)^{1/2}\tilde{x}] \qquad (A.5)$$

$$\phi(\tilde{x} \to -\infty) \approx q_C(\tilde{x})/q_B(\tilde{x}) \approx g_2 \exp\{[(\tilde{\chi}_{AC} - \tilde{\chi}_{BC}\phi_{B\infty}^2)^{1/2} - (\tilde{\chi}_{AB} - \tilde{\chi}_{BC}\phi_{C\infty}^2)]^{1/2}\tilde{x}\} \qquad (A.6)$$

Here g_1 and g_2 are proportionality constants to be determined as indicated below.

The approach to the equator, $\theta \to \pi/2$, corresponds to $\tilde{x} \to \infty$. The asymptotic analysis in this region is best carried out in θ,ϕ language. Here $\phi \to \alpha$ where $\cos^2 \alpha = \phi_{B\infty}$. We can write as equations valid asymptotically as $\tilde{x} \to \infty$:

$$\frac{d^2\theta}{d\tilde{x}^2} = -(\tilde{\chi}_{AB}\phi_{B\infty} + \tilde{\chi}_{AC}\phi_{C\infty} - \tilde{\chi}_{BC}\phi_{B\infty}\phi_{C\infty})(\pi/2 - \theta) \qquad (A.7)$$

$$\frac{d^2\phi}{d\tilde{x}^2} = 4\tilde{\chi}_{BC}\phi_{B\infty}\phi_{C\infty}(\alpha - \phi) \qquad (A.8)$$

The asymptotic solutions are

$$\theta(\tilde{x} \to \infty) \approx \frac{\pi}{2} - g_3 \exp[-(\tilde{\chi}_{AB}\phi_{B\infty} + \tilde{\chi}_{AC}\phi_{C\infty} - \tilde{\chi}_{BC}\phi_{B\infty}\phi_{C\infty})^{1/2}\tilde{x}] \qquad (A.9)$$

$$\phi(\tilde{x} \to \infty) \approx \alpha - g_4 \exp[-2(|\tilde{\chi}_{BC}|\phi_{B\infty}\phi_{C\infty})^{1/2}\tilde{x}] \qquad (A.10)$$

These asymptotic forms may be used to move the solutions away from $\tilde{x} \to \pm\infty$, far enough to avoid difficulty with the numerical integration, but not so far that the asymptotic forms are not excellent approximations. In this way the differential eqs 4.17 to 4.20 may be integrated from $\tilde{x} = -\infty$ toward the right and from $\tilde{x} = +\infty$ toward the left. The four constants, g_i, will be chosen so that the two solutions match at some point, which we chose as the point, call it x_h, where $\theta = \pi/4$. (Actually, in the beginning we regard $\tilde{x}_h$ as the zero of x. Later we shift the x axis, after we have a solution and can calculate the position of the Gibbs dividing surface relative to $\tilde{x}_h$.) Hence, the implicit equations for the g_i's are

$$\theta(\tilde{x} = \tilde{x}_h -) = \pi/4 \qquad (A.11)$$

$$\theta(\tilde{x} = \tilde{x}_h +) = \pi/4 \qquad (A.12)$$

$$p_\theta(\tilde{x} = \tilde{x}_h -) = p_\theta(\tilde{x} = \tilde{x}_h +) \qquad (A.13)$$

$$\phi(\tilde{x} = \tilde{x}_h -) = \phi(\tilde{x} = \tilde{x}_h +) \qquad (A.14)$$

These equations guarantee the continuity of p_ϕ at $\tilde{x}_h$ by the conservation of "energy".

One must start with a fairly good guess for the g_i's, or the trajectory will go off into physically meaningless regions of the sphere. We included in the program some methods of improving the guess when this occurred. A convenient change of variables if from $\tilde{x}$ to s defined by $s = (2/\pi) \arctan(e^{\tilde{x}})$. This is chosen so that for the A/B interface the solution is $\theta = (\pi/2)s$.

Appendix B: Solution Where the Ratio of B to C Remains Constant

The ratio $\phi_{B\infty}/\phi_{C\infty}$ will remain constant if $\phi(\tilde{x}) = \alpha$ and $p_\phi = 0$ for all $\tilde{x}$. From eq 4.20 we see that $dp_\phi/d\tilde{x}$ will everywhere vanish under these conditions if

$$\tilde{\chi}_{AC} - \tilde{\chi}_{AB} - \tilde{\chi}_{BC}(\phi_{B\infty} - \phi_{C\infty}) = 0 \qquad (B.1)$$

With $\phi(\tilde{x}) = \alpha$, eq 4.20 for $d\tilde{p}_\theta/d\tilde{x}$ reduces to ($\tilde{p} \equiv p/6^{-1/2}b$)

$$d\tilde{p}_\theta/d\tilde{x} = (\tilde{\chi}'/4)\sin(4\theta) \qquad (B.2)$$

$$\tilde{\chi}' = \tilde{\chi}_{AB}\phi_{B\infty} + \tilde{\chi}_{AC}\phi_{C\infty} + |\tilde{\chi}_{BC}|\phi_{B\infty}\phi_{C\infty} \qquad (B.3)$$

Equation B.2 is just the equation for a binary interface[1] with an effective $\tilde{\chi}$ given by $\tilde{\chi}'$. In view of eq B.1, $\tilde{\chi}'$ can also be written as

$$\tilde{\chi}' = \frac{(\tilde{\chi}_{AB} + \tilde{\chi}_{AC} + |\tilde{\chi}_{BC}|)^2 - 4\tilde{\chi}_{AB}\tilde{\chi}_{AC}}{4|\tilde{\chi}_{BC}|} \qquad (B.4)$$

Appendix C: Analytical Solution for Strong B Adsorption

In this appendix we will see what conditions lead to strong B adsorption. By this we mean (moving from left to right) $\phi_B(\tilde{x})$ goes nearly to unity for a range of $\tilde{x}$ before significant amounts of C appear. We will also examine the consequences of strong B adsorption. In section VI.B we stated conditions that would lead to the point of maximum acceleration of the ϕ variable occurring when the A concentration is small. Here we will elaborate on this, too.

Assume that there is a region, which we will call region I, where $\phi(\tilde{x})$ and $p_\phi(\tilde{x})$ are small. Then the energy equation, $K(x) + V(x) = 0$, provides a first-order equation for $\mathrm{d}\theta/\mathrm{d}\tilde{x}$:

$$\mathrm{d}\theta/\mathrm{d}\tilde{x} = (1/k)\Delta \sin \theta \tag{C.1}$$

$$k^2 = (\tilde{\chi}_{AB} + |\tilde{\chi}_{BC}|\phi_{C\infty}^2)^{-1} \tag{C.2}$$

$$\Delta = (1 - k^2 \sin^2 \theta)^{1/2} \tag{C.3}$$

The solution is

$$\tilde{x}_0 - \tilde{x} = \frac{k}{2}\left[\log \frac{\Delta + \cos\theta}{\Delta - \cos\theta} - \log \frac{\Delta_0 + \cos\theta_0}{\Delta_0 - \cos\theta_0}\right] \tag{C.4}$$

where sub 0 means evaluated at $\tilde{x}_0$, the boundary between regions I and II. One can evaluate $\cos\theta_0$ from eq 6.4. If we assume that ϕ_A falls from the value $\cos\theta_0$ precipitously to zero at $\tilde{x}_0$, then eq 2.4, which defines the Gibbs dividing surface for A to be at $\tilde{x} = 0$, yields as an equation for $\tilde{x}_0$:

$$\tilde{x}_0 = \log \frac{k+1}{k\cos\theta_0 + \Delta_0} \tag{C.5}$$

There is an important observation to be made for the case where $\tilde{\chi}_{AC} \rightarrow \infty$. The largest that θ_0 can get to be is $\pi/2$ so that as $\phi_A(\tilde{x}_0) \rightarrow 0$, one finds that

$$\lim_{\phi_A(\tilde{x}_0)\rightarrow 0} \tilde{x}_0 = \frac{1}{2}\log\frac{1+k}{1-k} \tag{C.6}$$

Unfortunately, this limit is approached rather slowly. For $\tilde{\chi}_{AC} = 8$, $\tilde{\chi}_{BC} = -0.25$, and $\phi_{B\infty} = 0.5$, one finds by eq C.6 that $\tilde{x}_0 = 2.094$, whereas eq C.5 yields $\tilde{x}_0 = 1.397$. Nevertheless, for the true asymptotic limit, eq C.6 can be used; and it tells us that the properties of the system are independent of $\tilde{\chi}_{AC}$ for large $\tilde{\chi}_{AC}$.

It is very easy to determine in closed form the contribution of region I to the system's properties. As we saw in the body of the paper, $\tilde{\gamma}$, $\tilde{a}_L$, and $\tilde{n}_{xsB}$ are given as integrals over $\tilde{x}$. These can be converted to integrals over θ using eq C.1. We report only the results:

$$\tilde{\gamma}_I = (1/k)(1 - \Delta_0\cos\theta_0) + |\tilde{\chi}_{BC}|\phi_{C\infty}^2\tilde{x}_0 \tag{C.7}$$

$$\tilde{a}_L = (1/k)(1 - \Delta_0\cos\theta_0) - |\tilde{\chi}_{BC}|\phi_{C\infty}^2\tilde{x}_0 \tag{C.8}$$

$$n_{xsB,I} = \phi_{C\infty}\tilde{x}_0 \tag{C.9}$$

The true limits, as conditions make $\theta_0 \rightarrow \pi/2$, are easily seen.

Next we should consider region II. Here we have assumed that there is no A, i.e., $\theta = \pi/2$ and $\mathrm{d}\theta/\mathrm{d}\tilde{x} = 0$. Now the conservation of energy gives an equation for ϕ

$$\mathrm{d}\phi/\mathrm{d}\tilde{x} = |\tilde{\chi}_{BC}|^{1/2}(\cos^2\phi - \cos^2\alpha) \tag{C.10}$$

with solution

$$\tan\phi = \tan\alpha \tanh\,[|\tilde{\chi}_{BC}|^{1/2}(\phi_{B\infty}\phi_{C\infty})^{1/2}(\tilde{x} - \tilde{x}_1)] \tag{C.11}$$

$$\tilde{x}_1 = \tilde{x}_0 - \frac{1}{2|\tilde{\chi}_{BC}|^{1/2}\cos\alpha\sin\alpha}\log\left[\frac{\tan\alpha + \tan\phi_0}{\tan\alpha - \tan\phi_0}\right] \tag{C.12}$$

Again $\tilde{x}_0$ is the dividing point between regions I and II, and $\phi_0 = \phi(\tilde{x}_0)$. For strict asymptotics one should assume that $\tilde{x}_0$ is given by eq C.6, and $\phi_0 = 0$. However, we have been trying in this appendix to give a reasonable way of estimating properties before the asymptotic range is reached. Thus, we will assume that the B concentration is continuous at $\tilde{x}_0$, so $\phi_0 = {}^1/_2\pi - \theta_0$. Unfortunately that also means that the A concentration falls suddenly to zero at $\tilde{x}_0$, while the C concentration jumps suddenly to such a value that it replaces the A.

Again, it is easy to evaluate in closed form the contribution to the interfacial tension and adsorption:

$$\gamma_{II} = |\tilde{\chi}_{BC}|^{1/2}[{}^1/_2\sin(2\alpha) - {}^1/_2\sin(2\phi_0) - (\alpha - \phi_0)\cos(2\alpha)] \tag{C.13}$$

$$n_{xsB,II} = \frac{\alpha - \phi_0}{|\tilde{\chi}_{BC}|^{1/2}} \tag{C.14}$$

References and Notes

(1) Helfand, E.; Tagami, Y. *J. Chem. Phys.* **1972**, *56*, 3592.

(2) Helfand, E.; Sapse, A. M. *J. Chem. Phys.* **1975**, *62*, 1327.

(3) Helfand, E. In *Polymer Compatibility and Incompatibility*; Solc, K., Ed.; MMI Press, Harwood Academic Publishers: New York, 1982. Helfand, E. *J. Chem. Phys.* **1975**, *62*, 999.

(4) Fredrickson, G. H. In *Physics of Polymer Surfaces and Interfaces*; Sanchez, I., Ed.; Butterworth: London, in press.

(5) Flory, P. J. *Principles of Polymer Chemistry*; Cornell University Press: Ithaca, NY, 1953.

(6) Halperin, A.; Pincus, P. *Macromolecules* **1986**, *19*, 79.

(7) Leibler, L. *Macromolecules* **1982**, *15*, 1283.

(8) LeGrand, D. G.; Gaines, G. L., Jr. *J. Colloid Interface Sci.* **1969**, *31*, 162. *Ibid.* **1975**, *50*, 272. *Ibid.* **1978**, *63*, 394. Wu, S. *Polymer Interface and Adhesion*; Marcel Dekker: New York, 1982. Anastasiadis, S. H.; Gancarz, I.; Koberstein, J. T. *Macromolecules* **1988**, *21*, 2980.

(9) Helfand, E.; Bhattacharjee, S. M.; Fredrickson, G. H. *J. Chem. Phys.* **1989**, *91*, 7200. Broseta, D.; Fredrickson, G. H.; Helfand, E.; Leibler, L. *Macromolecules* **1990**, *23*, 132.